



## Layered lithospheric mantle in the central Baltic Shield from surface waves and xenolith analysis

Marianne Bruneton<sup>a</sup>, Helle A. Pedersen<sup>a,\*</sup>, Pierre Vacher<sup>b</sup>, Ilmo T. Kukkonen<sup>c</sup>,  
Nicholas T. Arndt<sup>d</sup>, Sigward Funke<sup>e</sup>, Wolfgang Friederich<sup>e</sup>, Véronique Farra<sup>f</sup>  
SVEKALAPKO Seismic Tomography Working Group

<sup>a</sup>Laboratoire de Géophysique Interne et Tectonophysique, Observatoire des Sciences de l'Univers de Grenoble, Grenoble, France

<sup>b</sup>Laboratoire de Planétologie et Géodynamique, Université de Nantes, Nantes, France

<sup>c</sup>Geological Survey of Finland, Espoo, Finland

<sup>d</sup>Laboratoire de Géodynamique des Chaînes Alpines, Observatoire des Sciences de l'Univers de Grenoble, Grenoble, France

<sup>e</sup>Institut für Meteorologie und Geophysik, J.W. Goethe Universität, Frankfurt, Germany

<sup>f</sup>Département de Sismologie, Institut de Physique du Globe de Paris, Paris, France

Received 9 January 2004; received in revised form 30 June 2004; accepted 23 July 2004

Editor: R.D. van der Hilst

### Abstract

Information on the structure of the upper mantle comes from two main sources. Regional seismic studies provide indirect information on large portions of the lithosphere, and mantle xenoliths provide direct information about the composition and physical properties of the small regions sampled by kimberlites and other magmas. Fundamental mode Rayleigh wave arrival times at seismic stations of the SVEKALAPKO seismic experiment, with periods between 10.5 and 190 s, were inverted to obtain a regional average shear-wave velocity model in the central Baltic Shield to a depth of 300 km. This model is very well constrained except for the crust and immediately below the Moho. Calculated velocities are approximately 4% faster than in standard Earth models for the upper mantle down to 250-km depth. A low velocity zone that could define the base of the lithosphere is absent. We compared our seismically derived shear-wave velocities to models derived from the compositions of lherzolite and harzburgite xenoliths in Finnish kimberlites, sampled in regions where the geotherm is well constrained. The velocities are similar for depths between 160 and 300 km. For depths shallower than 160 km, our seismically derived velocities are slower than those from the petrologic models, and they have a positive gradient with depth in contrast with the negative gradient predicted for homogeneous material in this depth interval. Our data are best explained by a chemical layering of the lithospheric mantle: A layer with abnormally low

\* Corresponding author. LGIT-Maison des Géosciences, BP 53, 38041 Grenoble cedex 9, France. Tel.: +33 4 76 82 80 35; fax: +33 4 76 82 81 01.

E-mail addresses: [marianne.bruneton@obs.ujf-grenoble.fr](mailto:marianne.bruneton@obs.ujf-grenoble.fr) (M. Bruneton), [pedersen@obs.ujf-grenoble.fr](mailto:pedersen@obs.ujf-grenoble.fr) (H.A. Pedersen).

velocities in the upper part of the lithosphere apparently grades downwards into more normal peridotitic compositions. Possible candidates for the slow composition of the shallower mantle are metasomatized peridotites, or ultramafic cumulates or restites. © 2004 Elsevier B.V. All rights reserved.

*Keywords:* lithosphere; surface waves; xenoliths; shear-wave velocity; Baltic Shield

## 1. Introduction

Understanding the growth and stabilization of the earliest continents remains a challenge to Earth sciences. The development of thick lithospheric keels seems to have protected the continental crust against recycling into the mantle, but the mechanism and the timing of the stabilization of these continental roots remain largely unknown. To answer these questions, a more complete knowledge of the structure and composition of the cratonic lithosphere is required. Seismic studies provide information on the present structure of the mantle in terms of seismic velocities and lateral variations (for example, in South Africa, see [1]). Studies of mantle xenoliths provide a good complement because these rocks directly sample the mantle and yield direct information about its composition and physical properties [2,3]. In theory, a combination of the two approaches provides valuable constraints on the history and evolution of continents. In practice, however, seismic models are rarely sufficiently well constrained to provide reliable constraints on mantle composition. In this paper, we describe a project that used the array geometry of the SVEKALAPKO seismic experiment in the Baltic Shield to provide an unusually well-constrained model for the absolute seismic velocities in a shield area.

The Baltic Shield consists of an Archean nucleus, the Karelian province, flanked to the northeast by the late Archean Lapland-Kola domain and to the southwest by the Proterozoic Svecofennian mobile belt [4] (see Fig. 1). Its formation started some 3.5 Ga ago and continued through the Archean and Proterozoic with several orogenies, continental extensions and accretion events. The last recorded tectonic events are extensional. They were accompanied by the intrusion of the Rapakivi granitoids (1.65–1.54 Ga), and the deposition of the Subjotnian sandstone (1.2 Ga) [5]. This composite craton,

which is largely free of sedimentary cover and without noticeable reworking since the Proterozoic, was the site of the SVEKALAPKO project [6], an important element of the EUROPROBE program [7].

As part of this large European project, a two-dimensional seismic network was installed in southern

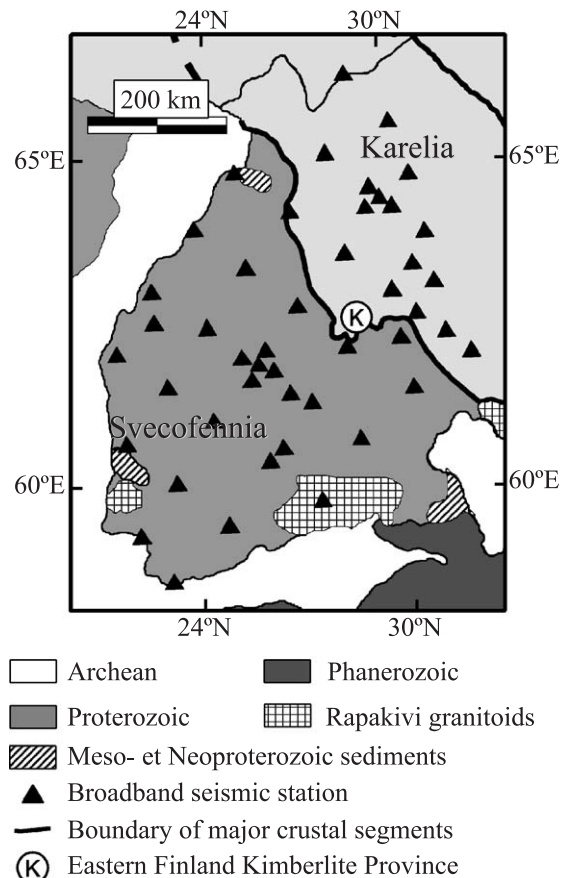


Fig. 1. Simplified geological map of the central Baltic Shield modified from [6]; triangles give the location of the broadband stations of the SVEKALAPKO array, location of the Eastern Finland Kimberlite Province is marked with the letter K.

Finland in the central part of the Baltic Shield [8]. It operated for 8 months, between summer 1998 and spring 1999. The network was composed of 144 seismic stations, out of which 46 were equipped with broadband sensors (43 CMG3 and STS2 with cutoff periods of 90 and 100 s, and 3 CMG40 with cutoff periods of 40 and 60 s; see Fig. 1). The concentration of 46 broadband seismic stations on a  $500 \times 800 \text{ km}^2$  area in the center of a shield provided a unique opportunity to obtain a very well constrained model of the local average shear-wave velocity with depth. The data set has been given to Orfeus and should be soon available on their website (Observatories and Research Facilities for European Seismology, <http://orfeus.knmi.nl>).

Using a newly developed surface wave tomography [9] and the arrival times of the teleseismic fundamental mode Rayleigh wave recorded by the 46 broadband stations, we obtained a 1D average shear-wave velocity model with depth for the central Baltic Shield. The presence of kimberlite pipes containing mantle xenoliths in the same area [10] makes it possible to compare velocities predicted from xenolith petrology with seismically derived velocities, and in so doing, to obtain constraints on the composition of the lithospheric mantle in the area.

## 2. Data selection and processing

For the present study, we used the fundamental mode Rayleigh wave recorded on the vertical component of the sensors. Due to the large number of different sensors and recorders, the data were first corrected for the instrument response. Then, a phase-matched filter [11] was used to extract the fundamental mode Rayleigh wave from the signal.

We selected 69 events that met the following criteria: a magnitude greater than 5.5, an epicentral distance larger than  $30^\circ$ , and a high-quality signal at most of the stations. On the filtered signals, we measured time delays between pairs of stations versus frequency using the phase of the Wiener filter [12]. For each station pair, we selected only very high quality data by eliminating points with a coherency lower than 0.95 or a signal to noise ratio lower than 4.

## 3. Average dispersion curve

We inverted the fundamental mode Rayleigh wave delay times of the SVEKALAPKO seismic experiment for an average phase velocity dispersion curve using the procedure of Bruneton et al. [9]. This method is based on two-dimensional paraxial ray tracing and aims at calculating the phase velocities that best explain the arrival times of the surface waves at all the stations. A novel aspect is that it takes into account the nonplanarity of incoming wavefronts. As the phase velocity depends on the frequency, one inversion per frequency is necessary. This method was developed to invert for lateral variations of phase velocity under a broadband array. To obtain the average velocity beneath the array, we imposed a constant velocity over the whole area for each frequency, but we still considered nonplane incoming waves because nearby heterogeneities may distort the wavefronts.

Although the cutoff period of most of the seismic stations is 90–100 s, the severe selection procedure of the data made it possible to retrieve reliable information for periods above 100 s. The number of inverted data is greatest for the 22.5-s period (1856 arrival times) but decreases at the longest periods (190 s: 557 arrival times). At shorter periods, the noise level increases and only 478 arrival times have a sufficient quality at 10.5 s. The dispersion curve obtained from

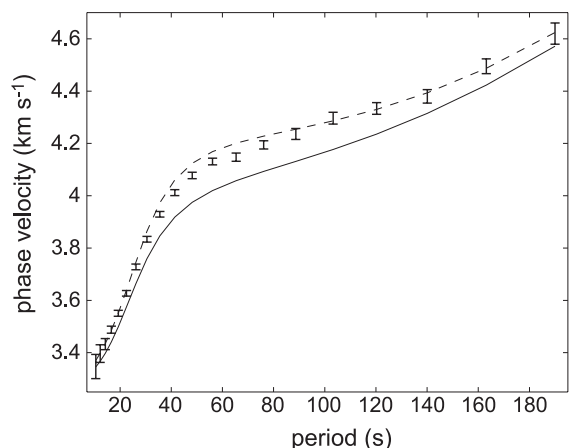


Fig. 2. Regional average dispersion curve (error bars), compared to the dispersion curves of different initial models for the inversion (solid line: ak135-derived model with three-layer crust; dashed line: xenoliths-derived model).

this data set, with error bars, is presented in Fig. 2. The computed error bars are proportional to the mathematical a posteriori covariance and to the inverse of the number of data.

#### 4. Inversion for shear-wave velocity

##### 4.1. Inversion method

We inverted the dispersion curve to obtain an average model of the shear-wave velocity with depth. This inversion follows a linearized method, by Maupin and Cara [13], which makes it possible to consider independent layers, each composed of velocities varying smoothly with depth. We used the program package developed by Saito [14] for the direct modeling and computation of the partial derivatives. The inversion algorithm [15] minimizes the square of the difference between the predicted and observed phase velocities. The inversion model contains only the shear-wave velocities: P-wave velocities, densities and depths of the interfaces are kept unchanged during the inversion. The influence of  $V_p$  and density on the inversion is small: For example, using a constant Poisson's ratio produces a similar S-wave velocity model.

Seismic surface wave dispersion cannot resolve small structures such as interfaces. We therefore impose velocity variations that are smooth over the entire upper mantle. However, at the end of this paper, we also tested a model with a strong interface in the middle of the lithosphere (Section 6). As in L ev eque et al. [16], the smoothness is controlled by the definition of a Gaussian correlation function. The correlation length is defined as the half width of the Gaussian for the 60% confidence interval. To reduce the nonuniqueness of the problem, we chose a large correlation length of 100 km. The a priori error in the initial velocity model is set to 4%, so that large variations from the initial model are possible. These two parameters control the smoothness of the result and the width of the error bars.

##### 4.2. Shear-wave velocity model

The initial shear-wave velocity model used in the inversion is based on the standard Earth model ak135

[17] for the mantle part, and on the work of Sandoval et al. [18] for the crust. Observed Moho depths vary between 38 and 64 km in the area of the SVEKA-LAPKO array. The thickest part of the crust exhibits a high-velocity lower crustal layer. We used an average crustal thickness of 51.2 km for the region under the array and placed the top of the high-velocity lower crust at 35-km depth. The crust above 35 km was arbitrarily separated in two equally thick layers. The influence of the crustal structure is discussed in Section 4.4. This initial model is plotted in Fig. 3 (Vs and phase velocity relative to the data in dashed black lines) and its associated dispersion curve is plotted in Fig. 2. In these figures, for most periods, the phase velocities of the initial model are 0.05 to 0.1 km s<sup>-1</sup> lower than the observed phase velocities. This is a first indication that the mantle has higher shear-wave velocities than ak135.

The model obtained after inversion is plotted in Fig. 3 (solid black line). The obtained phase velocities are consistent with the observed dispersion curve for all periods. The root mean square (rms) fit to the observed phase velocities equals 0.0095 km s<sup>-1</sup>.

This model was constructed from surface waves with wavelengths between 40 and 900 km. Because of anelasticity, the seismic velocities depend on the frequency and a correction is necessary before they

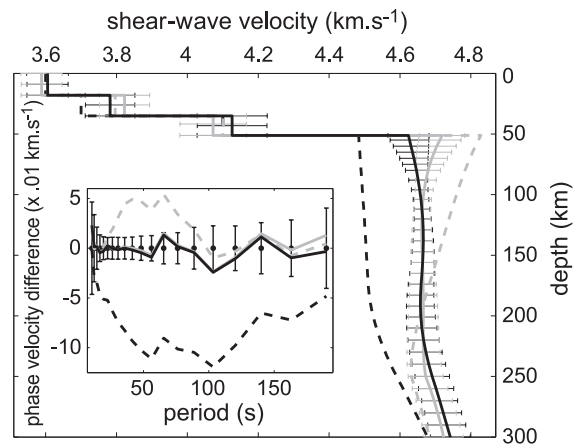


Fig. 3. Shear-wave velocity models: influence of the initial mantle structure. Dashed lines: initial models for the inversions; solid lines: final models; black: mantle model based on ak135 [17]; grey: mantle model based on a xenolith sample from Eastern Finland [10]. The insert shows the corresponding phase velocity dispersion curve in km s<sup>-1</sup> relative to the data.

can be compared with velocities obtained using other methods. The correction was made according to Eq. (5.81) of Aki and Richards [19] using a reference frequency of 1 Hz. As the data were obtained from frequencies lower than the reference, correcting for a high attenuation (low  $Q$  value) increases the velocities. Observed  $Q$  values for long-period seismic waves in the continental lithosphere range from 125 to almost 1000 [20–22]. We adopted a two-layer  $Q$  model following the standard Earth model ak135-f [23]. In this model  $Q=600$  for the crust and  $Q=400$  for the lithosphere, which is assumed to extend to 300-km depth. From geobarometric studies of xenoliths, the thickness of the lithosphere in the Baltic Shield is thought to be at least 250 km [24]. Furthermore, no clear low-velocity zone could be attributed to the lithosphere–asthenosphere boundary in our seismic model down to 300-km depth (Fig. 3). Fig. 4 shows the influence of the correction for anelasticity using different attenuation values in the lithosphere. Modifying  $Q$  from 1000 to 100 produces variations of  $V_s$  in the mantle of 1.1–1.6%; at larger depths, the difference is higher. However, the curves with constant  $Q$  are almost parallel and an attenuation value with  $Q$  lower than 200 does not seem realistic for a cratonic lithosphere.

In the shear-wave velocity model of Fig. 3, velocities are higher (by about 4%) than standard

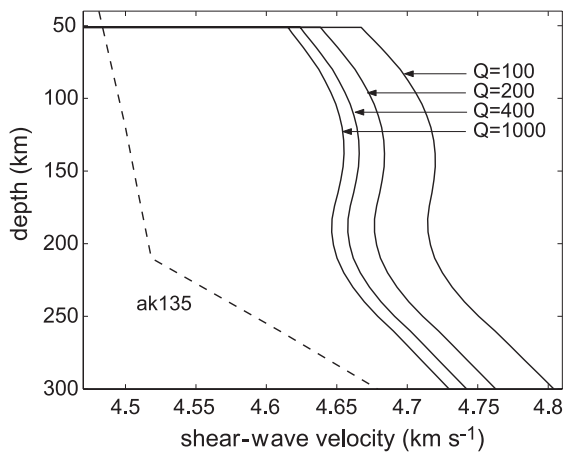


Fig. 4. Influence of the correction for anelasticity on the seismic model. Solid lines: shear-wave velocity models derived from the Rayleigh waves dispersion curve with different values of the quality factor  $Q$  for the upper mantle; grey dashed line: standard Earth model ak135 [17].

Earth model ak135 [17] for the mantle down to 250 km. There is no resolvable low-velocity zone: The base of the lithosphere is not clearly defined in this shear-wave velocity model.

#### 4.3. Influence of the input parameters

To test the influence of the input parameters for the inversion (correlation length and a priori error in the velocity model), we ran a second series of inversions in which the correlation length was varied between 100 and 20 km, and the a priori error between 2% and 4%.

The difference in rms fit to the data dispersion curve for these inversions is insignificant as it varies between 0.0089 and 0.0095  $\text{km s}^{-1}$ . The average difference of  $V_s$  is less than 0.5% for all models. Increasing the a priori error or decreasing the correlation length leads to larger variations in shear wave velocity and larger a posteriori error bars. Reducing the smoothing of the model also results in an upward translation of the velocity oscillations in the mantle. However, as the velocity variations remain small, this translation does not alter the overall aspect of the model.

We chose a value of 4% for the a priori error in the velocity model and 100 km for the correlation length, values we believe give realistic error bars but avoid too great an influence from the initial model. The final error bars (Fig. 3) are of the order of 1% at 100–200-km depth and up to 2% elsewhere in the mantle.

#### 4.4. Influence of crustal structure

An interpretation that combines seismic and gravity data in the same region led Kozlovskaya et al. [25] to define a four-layered rather than a three-layered crust. Based on their results, we inverted the data using a different initial model composed of the same ak135-based mantle structure and of four crustal layers with the following thicknesses (from top to bottom): 15, 13, 7, and 16.2 km.

The rms fit to the data of the resulting model is only slightly better than for the previous inverse model (0.0085  $\text{km s}^{-1}$ ). Although the velocities within the crust depend strongly on the number and thickness of the layers, the mantle structure is unchanged. It appears that our data cannot resolve



the crustal structure but its modification does not alter the result obtained for the mantle.

However, the constant Moho depth imposes a strong constraint on the shear-wave velocity model. Thanks to the numerous seismic sounding profiles in the region, and confirmed by gravity data [25], the Moho depth is known to within 2 km (Kozlovskaya, personal communication). We therefore tested the influence of an increase of 3 km in the Moho depth, as this is higher than the maximum error that can be expected on the average Moho depth. This resulted in an increase in the velocity in the lower crustal layer of 0.75%. Immediately below the Moho, mantle velocities increased by 0.5%, an effect that became negligible around 100–120 km. Such a small variation in the shallow mantle does not influence the overall shape of the velocity profile. More realistic errors (<1 km) have an insignificant influence on mantle velocities.

#### 4.5. Influence of the initial mantle structure

We also changed the initial mantle structure while keeping a three-layer crust. Recently, Kukkonen et al. [24] computed a seismic velocity model on the basis of the compositions of mantle xenoliths from eastern Finland. Because they did not take into account anelasticity, we recalculated the S-wave velocities versus depth based on the original xenolith compositions [10], and taking into account anelasticity and updated data from laboratory experiments. The initial model corresponds to a garnet harzburgite (composi-

tion 2 of Table 1) and the method for computing the seismic velocities is given in more detail in Section 5.1. This model is plotted in Fig. 3 ( $V_s$  and phase velocity relative to the data in dashed grey lines) and its associated dispersion curve is plotted in Fig. 2.

The resulting model is shown in Fig. 3 (solid grey line). Its dispersion curve (insert of Fig. 3) is close to the data for the entire measured interval. After inversion, the rms fit to the phase velocity data is  $0.0092 \text{ km s}^{-1}$ .

The two final models plotted in Fig. 3 are quite similar, particularly at the depths of origin of the xenolith sample (~210 km). However, there are significant differences at 50–80-km depth where higher(lower) velocities are compensated by lower(higher) velocities in the lowermost crust. It is difficult to choose between the two models because the velocity variations are so small that they are not resolved by other seismic data. Even though the shallowest mantle velocities are somewhat dependent on the initial model, the mantle velocities from 100 to 300 km are particularly robust.

## 5. Comparison with xenolith-derived velocities

### 5.1. Computation of seismic velocities from xenolith compositions

From a petrologic point of view, the seismic velocities depend on the density and elastic param-

Table 1  
Composition of mantle rocks<sup>a</sup> (% in volume)

Rock type	OL (Mg#)	OPX	CPX	GT	SP	AMPH	PHL	Reference
(1) GT-SP harzburgite	70.0 (0.95)	25.2	0.9	2.7	–	–	–	[10] L48
(2) GT harzburgite	86.1 (0.95)	10.4	1.0	2.5	–	–	–	[10] L29
(3) GT lherzolite	64.2 (0.95)	26.4	8.1	1.2	–	–	–	[10] L66
(4) GT OL websterite	14.3 (0.95)	77.3	7.3	1.0	–	–	–	[10] L29
(5) GT wehrlite	75.6 (0.88)	1.5	18.2	4.7	–	–	–	[10] L44
(6) AMPH peridotite	59.0 (0.85)	21.0	15.0	–	2.0	3.7	–	[36]
(7) AMPH peridotite	50.0 (0.82)	17.0	21.0	–	1.5	10.0	–	[37]
(8) PHL peridotite	53.0 (0.90)	–	32.0	–	1.0	–	13.0	[38]
(9) granit. m. rest.	30.0 (0.80)	–	60.0	10.0	–	–	–	[39]

Reference for the Finnish xenoliths also contains the sample name.

<sup>a</sup> OL: olivine (forsterite–fayalite); OPX: orthopyroxene (enstatite–ferrosilite); CPX: clinopyroxene (diopside–edenbergite); GT: garnet (pyrope–almandin); SP: spinel; AMPH: amphibole; PHL: phlogopite; granit. m. rest.: granitoid magma restite. For computations in this paper, we assumed that the Mg# in both pyroxenes is equal to that of olivine, and the Mg# in garnet is twice that of olivine. For the elastic parameters of amphibole and phlogopite, we used published laboratory analysis of minerals from the same family (hornblende and biotite).

ters, which in turn depend on the rock composition, the orientation of minerals, and finally on temperature and pressure conditions. We computed the seismic velocities following Goes et al. [26]. In this method, values of density and elastic parameters at ambient conditions are extrapolated to high  $P$ – $T$  conditions for each mineral, then properties are averaged out using a Voigt–Reuss–Hill procedure. Finally, computed seismic velocities are corrected of anelasticity (see below). Reference values for the elastic parameters of the minerals, as well as their pressure and temperature derivatives, are based on laboratory experiments (see [26] for olivine, orthopyroxene, clinopyroxene, garnet and spinel, and [27] for phlogopite and amphibole).

As each of the elastic parameters is known within a certain error [26], we also calculated for composition 2 (Table 1) the maximum and minimum predicted velocities at each depth. The variation ranges from  $\pm 0.5\%$  at 50-km depth to  $\pm 2.1\%$  at 250-km depth. These variations are quite large but all curves have (1) a significant negative velocity gradient with depth within the lithosphere, (2) a low-velocity region at the base of the lithosphere, and (3) a positive gradient below 250-km depth, where the geotherm becomes convective.

For the computations, we used the pressure profile of PREM [28]. We used the geotherm derived by Kukkonen et al. [24] based on a two-dimensional conductive model along a seismic profile in the Finnish kimberlite province [10,29]. This geotherm is in satisfactory agreement with the thermobarometry of the xenolith samples (less than 100 °C discrepancy except for three samples). Measurements of surface heat flow coupled with geochemical analysis of heat-producing elements [30] support the idea of uniform upper mantle temperatures beneath Finland. The study of receiver functions shows horizontal interfaces at the seismic boundaries of 410 and 670 km [31], which also implies homogeneous upper-mantle temperatures. Both interfaces are slightly shallower than the global average depth indicating a cold mantle above these interfaces. Based on these studies, the geotherm in this cratonic setting is not likely to have been modified by more than 100° since the time of eruption of the kimberlites. A modification of the geotherm by  $\pm 100$  °C shifts the predicted  $V_s(z)$  to higher or lower velocities (maximum variation 1.2%), without chang-

ing significantly the shape of the model. The change in velocity gradient at 250-km depth is located at our predefined base of the lithosphere. A different lithospheric thickness has a negligible effect on the shape of the predicted  $V_s(z)$  within the lithosphere.

The predicted seismic velocities were corrected for anelasticity on the basis of a mineralogical interpretation of the quality factor  $Q$ , which depends on pressure, temperature, and several thermodynamic factors [26]. Note that these theoretical models are generally different from the  $Q$  models used for correcting the observed  $V_s$  (see Section 4.2). We used the model  $Q_1$  of Goes et al. [26]. As the variation of  $Q$  with depth is somewhat uncertain (especially because of the activation volume), we tested the effect of adopting the same constant  $Q$  model that we used for correction of the seismic model. A  $Q$  of 400 at all depths slightly reduces the velocity gradients: It yields lower velocities in the uppermost mantle (maximum discrepancy 0.5%) and higher velocities around 250 km depth (maximum discrepancy 0.7%), improving the fit to our seismic observations. Nonetheless, the predicted shear-wave velocities in the lithosphere always show a negative gradient with depth.

The predicted velocities we obtain from these computations are faster than the recent study conducted on shield xenoliths of South Africa by James et al. [32]. The rock compositions and the geotherms of the two studies are very similar and do not influence largely the results. The correction for anelasticity decreases the velocities of the lowermost lithosphere, thereby enhancing slightly the negative velocity gradient. Most of the difference between the two studies is explained by the different elastic parameters used. Because HT-HP laboratory experiments have progressed significantly in the last 10 years, we preferred the more recent compilation of Goes et al. [26] to the compilation of Bass [33] used by James et al. [32].

### 5.2. Mantle xenoliths from eastern Finland

In the region covered by the SVEKALAPKO seismic array, mantle xenoliths that provide constraints on the mantle composition are restricted to a single location within the Archean domain, close to the limit with the Proterozoic domain [10] (see Fig. 1).

Most of the sampled xenoliths are common peridotites such as harzburgite and lherzolite, and only a few have more unusual compositions. We selected five compositions that represent the maximum range of shear-wave velocities predicted using the samples described by Kukkonen and Peltonen [10]. Most xenoliths originate from the garnet facies (180–240-km depth). They are, in order of abundance, lherzolite (composition 3 Table 1), harzburgite (composition 2), wehrlite (composition 5), and websterite (composition 4). The remaining xenoliths are strongly depleted harzburgite from the spinel–garnet facies (110–180-km depth). Composition 1 leads to the fastest velocities in this group of samples.

The profiles based on the composition of harzburgites and lherzolites (1–3) provide anomalously high phase velocities for the period range 30–80 s, which corresponds to the depth interval 40–150 km (the dispersion curve computed from composition 2 is shown in Fig. 2 and in the insert of Fig. 3). To better understand this discrepancy, we compare the observed and predicted shear-wave velocity models in Fig. 5.

There are major differences between the shapes of the two types of profile. The velocity curves based on the compositions 1–3 have a negative velocity gradient for the lithosphere whereas the profiles based on seismic observations have an almost constant

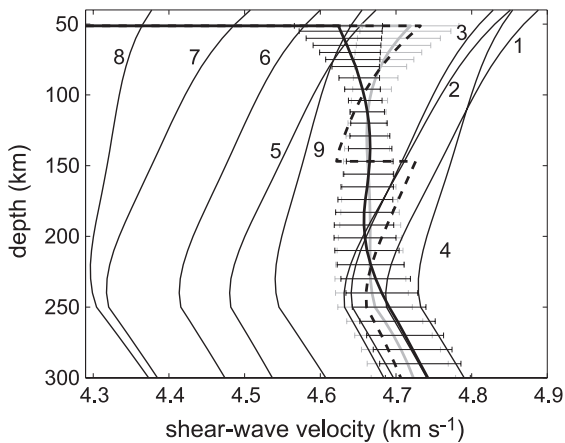


Fig. 5. Comparison between surface wave derived mantle velocities (bold lines with error bars), and computations based on rock composition (thin black lines with associated number, see Table 1): 1–5: selected xenoliths from Eastern Finland [10], 6 to 8: hydrated peridotites [35–37]; 9: residue of granitoid formation [38]. The dashed black line corresponds to a mantle with two noncorrelated layers.

velocity. The gradients become comparable for depths larger than 250 km, corresponding to the asthenosphere in the geotherm that we used. This supports our choice of lithospheric thickness.

For depths below 160 km, the observed shear-wave velocities are similar to the velocities calculated from common peridotite compositions. This is the part of the lithospheric mantle from which the majority of the xenoliths originate. Above 160 km, velocities predicted from the harzburgite and lherzolite compositions are faster than the observations. Moreover, the peridotite from the spinel–garnet facies (composition 1), representing the shallowest xenoliths, exhibits even faster velocities. The lithosphere sampled by the kimberlites therefore does not appear representative of the whole region sampled by the seismic waves, and we had to consider other compositions to explain the seismic observations.

The velocities computed from composition 4 (websterite) are comparable to those of compositions 1–3 (Fig. 5), and they cannot explain the slow upper mantle. The presence of wehrlite (composition 5) would lower the velocity of the mantle (Fig. 5), but large accumulations of such a rock are unlikely [34].

Mantle eclogites are less common in the eastern Finland xenoliths and none of these samples was fresh enough for geochemical analysis [10]. The velocity predicted from a hypothetical cratonic eclogite (50% garnet, 50% omphacite [32]) is faster than our seismic model. Even though some eclogites with unusual composition could produce lower velocities, it appears unlikely that they explain our observations over this large area.

### 5.3. Exotic compositions

In Fig. 5, we included the shear-wave velocity models obtained from further four different rock compositions (compositions 6–9, see Table 1) known to have low seismic velocities.

Compositions 6 to 8 represent strongly hydrated peridotites [35–37]. They correspond to mantle material metasomatized to different degrees and by different fluids. All three compositions give velocities that are lower than those of our seismic model (Fig. 5). Our seismic data could therefore be explained by the presence of only moderately metasomatized



peridotite, i.e., rock containing less phlogopite or amphibole than the chosen examples.

Finally, we tested a composition (9) proposed by Arndt and Goldstein [38], which corresponds to an olivine+clinopyroxene+garnet restite left in the lower crust following melting that gave rise to granitoid magmas. Such a restite has a density greater than that of the surrounding crust and should accumulate at the top of the lithospheric mantle. This composition produces the shear-wave velocity profile that is the closest to our seismic model. A composition with slightly more garnet or less clinopyroxene would match the data.

## 6. Discussion and conclusions

The seismic array of the SVEKALAPKO seismic experiment is located on two different crustal units, the Archean and the Proterozoic, with the later representing two thirds of the study area (Fig. 1). Both surface wave and body wave tomography show, however, that the lithospheric structure is not simple [39,40], in contrast to results from South Africa, for example [1]. The presented regional model therefore integrates over lateral heterogeneities, but it is the best resolved absolute Vs model known within a shield area. Our main conclusions may not apply to the entire region, but a stratified lithosphere must be a dominant feature.

The presence of depth-dependent anisotropy would not modify noticeably our conclusions. Our model, constructed from Rayleigh waves, is influenced mainly by the vertical component of S-wave velocity. Explaining lower than predicted Sv velocities in the upper part of the lithosphere by anisotropy alone would require a horizontal fast axis in this layer and a perfectly aligned vertical fast axis in the lower lithosphere. Based on tectonic interpretation of the anisotropy, such a situation is very unlikely; and an oblique fast axis would not produce velocity variations large enough to explain our observations.

The observed velocities are approximately 4% higher than the standard Earth model ak135 [17] in the upper 200 km of the mantle. They also lack a clear low-velocity zone that could define the base of the lithosphere.

By testing different initial models, we conclude that the structure of the crust is not resolved by our data. The velocity of the mantle down to 80-km depth is also

somewhat uncertain as it shifts by 1.5% when different initial models are used. A well-constrained, independently derived shear-wave velocity model for the crust would improve the resolution in the uppermost mantle.

The seismically derived shear-wave velocities are similar to models computed from the petrology of lherzolite and harzburgite xenoliths from eastern Finland for the depth of origin of most samples (160–240 km). For shallower depths, the fit is poor. The inferred velocities above 150 km are too slow to be consistent with material with the same composition as that in the lower part of the lithosphere. Moreover, the observed shear-wave velocity gradient varies between slightly positive or slightly negative, whereas a constant composition should give a strongly negative gradient.

Most of the xenoliths sampled in eastern Finland came from depths between 160 and 240 km; only two came from 100–150 km, and none from shallower depths. Although a paucity of samples from the shallower mantle appears to be widespread in cratonic areas [41,42], the reason for this is uncertain. Perhaps the upper part of the mantle has a composition that makes it less likely to be sampled by ascending kimberlite magmas.

To explain these observations, we propose a stratified lithospheric mantle in which a layer of anomalous and slow material overlies normal cratonic peridotite. To test if the surface wave analysis can discriminate between a model with two noncorrelated layers and a model with continuous variations of the velocity, we tested an initial Vs(z) model for the inversion with an interface at 150-km depth. The shear-wave velocities that result from this exercise depend highly on the initial model. However, at least one of the acceptable models appears to be consistent with the superposition of two internally homogeneous layers with different compositions (dashed black line, Fig. 5). The observed dispersion curve cannot discriminate between a continuously varying lithosphere and a stratification with sharp interfaces.

At least two petrologic processes might explain the lower velocities of the upper layer.

### 6.1. Mantle metasomatism

Mantle metasomatism produces mineral assemblages that are relatively rich in seismically slow

minerals such as Fe-rich olivine or pyroxene, clinopyroxene (rather than orthopyroxene), and hydrous phases. The causes of the process are diverse but in most cases they are linked to the upward migration of liquids, either silicate magmas or H<sub>2</sub>O/CO<sub>2</sub>-rich fluids. One geodynamic context in which this takes place is above a subduction zone where fluids liberated from dehydrating oceanic crust invade the overlying mantle wedge; another is the base of the lithosphere, which is subject to a constant flux of fluids from deeper sources.

The Baltic Shield has had a complex history. A succession of subduction events, collisions, accretions of island-arcs, terrains, and micro-continents [43] could have introduced fluids and created regions in the lithosphere with slower than normal seismic velocities. The problem with this type of explanation in the context of our seismic models is that it is normally the lower part of the lithosphere that becomes metasomatized, whereas our seismic data show a low-velocity layer in the upper part. Unless a layer of mantle material with “normal” seismic characteristics was added to the base of the lithosphere after a metasomatic event, we cannot see how this process could explain our data.

### 6.2. High-density ultramafic cumulates or residues in the upper part of the lithosphere

Two processes might provide an alternative explanation by producing low-velocity ultramafic cumulates or restites at the top of the lithospheric mantle [38,44,45]. First, dense picritic magmas may be trapped at the base of the crust, where they differentiate to form layered sills with gabbroic upper parts and olivine+pyroxene cumulate lower parts. The gabbroic layers are integrated into the crust while the cumulates return to the mantle due to their high density. Second, granitoid magmas formed during intracrustal melting leave dense residues that may also return to the mantle. These processes yield an anomalous layer in the upper lithosphere, which is richer in clinopyroxene and contains more Fe-rich olivine than normal cratonic lithosphere.

We have calculated the proportion of ultramafic restite mixed with cratonic peridotite required to reproduce our seismic observation. A shallow litho-

spheric layer containing 60–65% of restite (composition 9) and 35–40% of lherzolite or harzburgite (composition 2 or 3) is consistent with our observations. The composition evolves with depth (gradually or across sharp interfaces) into normal cratonic peridotite around 200 km.

This scenario also explains the anomalous crust of central Finland, which reaches 65-km thickness at places with a very high velocity lower crust but without topographic and gravity variations [18,25]. The high-velocity layer may consist of a complex of sills of essentially basaltic compositions, and the underlying layer in the upper part of the lithosphere could be the residues left by differentiation of these sills, or by the partial melting and magmatic evolution that produced the granitic portions of the Fennoscandian craton.

### Acknowledgments

We thank Tellervo Hyvönen for her help during the field work, as well as the numerous people who took part in it. The French participation received financial support from the “Intérieur de la Terre” program of INSU and used Lithoscope and RLBM seismic stations. We thank Valérie Maupin and Jean-Jacques Lévêque for the dispersion-curve inversion code and Senen Sandoval for the Moho depth model. This paper highly benefited from constructive reviews by Dr. S. Goes and Dr. W.L. Griffin. The European Science Foundation financed most of the workshops of the SVEKALAPKO project. Most of the computations presented in this paper were performed at the “Service Commun de Calcul Intensif de l’Observatoire de Grenoble” (SCCI). We used SAC for the treatment of the seismograms.

### References

- [1] D.E. James, M.J. Fouch, J.C. VanDecar, S. van der Lee, Kaapvaal Seismic Group, Tectospheric structure beneath southern Africa, *Geophys. Res. Lett.* 28 (2001) 2485–2488.
- [2] F.R. Boyd, Compositional distinction between oceanic and cratonic lithosphere, *Earth Planet. Sci. Lett.* 96 (1989) 15–26.
- [3] D.G. Pearson, G.J. Irvine, R.W. Carlson, M.G. Kopylova, D.A. Ionov, The development of lithospheric keels beneath the earliest continents: time constraints using PGE and Re–Os isotope systematics, in: C.M.R. Fowler, C.J. Ebinger, C.J.

- Hawkesworth (Eds.), *The Early Earth: Physical, Chemical and Biological Development*, Geological Society, London, 2002, pp. 65–90. Special Publication 199.
- [4] R. Gorbatshev, S. Bogdanova, *Frontiers in the Baltic Shield, Precambrian Res.* 64 (1993) 3–21.
- [5] A. Korja, T. Korja, U. Luosto, P. Heikkinen, Seismic and geoelectric evidence for collisional and extensional events in the Fennoscandian Shield—implications for Precambrian crustal evolution, *Tectonophysics* 219 (1993) 129–152.
- [6] S.-E. Hjelt, J.S. Daly, SVEKALAPKO, evolution of Paleoproterozoic and Archean lithosphere, in: D.G. Gee, H.J. Zeyen (Eds.), *EUROPROBE 1996—Lithosphere Dynamics: Origin and Evolution of Continents*, EUROPROBE Secretariat, Uppsala University, Sweden, 1996, pp. 57–67.
- [7] D.G. Gee, H.J. Zeyen (Eds.), *EUROPROBE 1996—Lithosphere Dynamics: Origin and Evolution of Continents*, EUROPROBE secretariat, Uppsala University, Sweden, 1996, 138 pp.
- [8] G. Bock, SVEKALAPKO Seismic Tomography Working Group, Seismic Probing of the Fennoscandian lithosphere, *EOS Trans. AGU* 82 (2001) 621, 628–629.
- [9] M. Bruneton, V. Farra, H.A. Pedersen, SVEKALAPKO Seismic Tomography Working Group, Non-linear surface wave phase velocity inversion based on ray theory, *Geophys. J. Int.* 151 (2002) 583–596.
- [10] I.T. Kukkonen, P. Peltonen, Xenolith-controlled geotherm for the central Fennoscandian Shield: implications for lithospheric–asthenospheric relations, *Tectonophysics* 304 (1999) 301–315.
- [11] A.V. Lander, A.L. Levshin, Recording, identification, and measurement of surface wave parameters, in: V.I. Keilis-Borok (Ed.), *Seismic Surface Waves in Laterally Inhomogeneous Earth*, Kluwer Academic Publishers, Dordrecht, 1989, pp. 131–182.
- [12] N. Wiener, *Time Series*, M.I.T. Press, Cambridge, MA, 1949, 739 pp.
- [13] V. Maupin, M. Cara, Love–Rayleigh wave incompatibility and possible deep upper mantle anisotropy in the Iberian peninsula, *Pure Appl. Geophys.* 138 (1992) 429–444.
- [14] M. Saito, *Disper 80*: a subroutine package for the calculation of seismic modes solutions, in: D.J. Doornbos (Ed.), *Seismological Algorithms*, Academic Press, New York, 1988.
- [15] A. Tarantola, B. Valette, Generalized nonlinear inverse problems solved using the least square criterion, *Rev. Geophys. Space Phys.* 20 (1982) 219–232.
- [16] J.-J. Lévêque, M. Cara, D. Roulard, Waveform inversion of surface wave data: test of a new tool for systematic investigation of upper mantle structures, *Geophys. J. Int.* 104 (1991) 565–581.
- [17] B.L.N. Kennett, E.R. Engdhal, R. Buland, Constraints on seismic velocities in the Earth from traveltimes, *Geophys. J. Int.* 122 (1995) 108–124.
- [18] S. Sandoval, E. Kissling, J. Ansgore, SVEKALAPKO Seismic Tomography Working Group, High-resolution body wave tomography beneath the SVEKALAPKO array: I. a priori 3D crustal model and associated traveltime effects on teleseismic wavefronts, *Geophys. J. Int.* 153 (2003) 75–87.
- [19] K. Aki, P.G. Richards, *Quantitative Seismology*, 2nd ed., University Science Books, Sausalito, CA, 2002, 700 pp.
- [20] Z.A. Der, A.C. Lees, V.F. Cormier, Frequency dependence of  $Q$  in the mantle underlying the shield of Eurasia, part III, The  $Q$  model, *Geophys. J. R. Astron. Soc.* 87 (1986) 1103–1112.
- [21] J.K. Xie, B.J. Mitchell, A back-projection method for imaging large-scale variations of  $L_g$  coda  $Q$  with application to continental Africa, *Geophys. J. Int.* 100 (1990) 161–181.
- [22] B.J. Mitchell, Anelastic structure and evolution of the continental crust and upper mantle from seismic surface wave attenuation, *Rev. Geophys.* 33 (1995) 441–462.
- [23] J.P. Montagner, B.L.N. Kennett, How to reconcile body-wave and normal-mode reference Earth model? *Geophys. J. Int.* 125 (1996) 229–248.
- [24] I.T. Kukkonen, K. Kinnunen, P. Peltonen, Mantle xenoliths and thick lithosphere in the Fennoscandian Shield, *Phys. Chem. Earth* 28 (2003) 349–360.
- [25] E. Kozlovskaya, S. Elo, S.-E. Hjelt, J. Yliniemi, M. Pirttijärvi, SVEKALAPKO Seismic Tomography Working Group, 3D density model of the crust of southern and central Finland obtained from joint interpretation of SVEKALAPKO crustal P-wave velocity model and gravity data, *Geophys. J. Int.* DOI: 10.1111/j.1365-246X.2004.02363.X.
- [26] S. Goes, R. Govers, P. Vacher, Shallow mantle temperatures under Europe from  $P$  and  $S$  wave tomography, *J. Geophys. Res.* 105 (2000) 11153–11169.
- [27] S.V. Sobolev, A.Y. Babeyko, Modeling of mineralogical composition, density and elastic wave velocities in anhydrous magmatic rocks, *Surv. Geophys.* 15 (1994) 515–544.
- [28] A.M. Dziewonski, D.L. Anderson, Preliminary reference Earth model, *Phys. Earth Planet. Inter.* 25 (1981) 297–356.
- [29] I.T. Kukkonen, A. Jöeleht, Geothermal modelling of the lithosphere in the central Baltic Shield and its southern slope, *Tectonophysics* 255 (1996) 24–45.
- [30] I.T. Kukkonen, Heat-flow map of northern and central parts of the Fennoscandian Shield based on geochemical surveys of heat producing elements, *Tectonophysics* 225 (1993) 3–13.
- [31] A. Alinaghi, G. Bock, R. Kind, W. Hanka, K. Wylegalla, TOR and SVEKALAPKO Groups, Receiver function analysis of the crust and upper mantle from the North German Basin to the Archean Baltic Shield, *Geophys. J. Int.* 155 (2003) 641–652.
- [32] D.E. James, F.R. Boyd, D. Schutt, D.R. Bell, R.W. Carlson, Xenolith constraints on seismic velocities in the upper mantle beneath Southern Africa, *Geochem. Geophys. Geosyst.* 5 (2004) Q01002, doi:10.1029/2003GC000551.
- [33] J.D. Bass, Elasticity of minerals, glasses, and melts, in: T.J. Ahrens (Ed.), *Mineral Physics and Crystallography: A Handbook of Physical Constants*, AGU Reference Shelf, vol. 2, AGU, Washington, D.C., 1995, pp. 46–63.
- [34] D.G. Pearson, D. Canil, S.B. Shirey, Mantle samples included in volcanic rocks: xenoliths and diamonds, in: R.W. Carlson (Ed.), *Treatise on Geochemistry, The Mantle and Core*, vol. 2, Elsevier Science, Amsterdam, 2003, pp. 171–275.
- [35] D.A. Ionov, U. Kramm, H.G. Stosch, Evolution of the upper mantle beneath the southern Baikal rift zone; an Sr–Nd isotope study of xenoliths from the Bartoy volcanoes, *Contrib. Mineral. Petrol.* 111 (1992) 235–247.

- [36] J.E. Nielson, J.R. Budahn, D.M. Unruh, H.G. Wilshire, Actualistic models of mantle metasomatism documented in a composite xenolith from Dish Hill, California, *Geochim. Cosmochim. Acta* 57 (1993) 105–121.
- [37] A.D. Edgard, F.E. Lloyd, D.M. Forsyth, L.R. Barnett, Origin of glass in upper mantle xenoliths from Quaternary volcanics of Gees, West Eifel, Germany, *Contrib. Mineral. Petrol.* 103 (1989) 277–286.
- [38] N.T. Arndt, S.L. Goldstein, An open boundary between lower continental crust and mantle: its role in crust formation and crustal recycling, *Tectonophysics* 161 (1989) 201–212.
- [39] S. Sandoval, E. Kissling, J. Ansorge, SVEKALAPKO Seismic Tomography Working Group, High-resolution body wave tomography beneath the SVEKALAPKO array: II. Anomalous upper mantle structure beneath central Baltic Shield, *Geophys. J. Int.* 157 (2004) 200–214.
- [40] M. Bruneton, H.A. Pedersen, V. Farra, N.T. Arndt, P. Vacher, SVEKALAPKO Seismic Tomography Working Group, Complex lithospheric structure under the central Baltic Shield from surface wave tomography, *J. Geophys. Res.* (2004) (in press).
- [41] W.L. Griffin, S.Y. O'Reilly, C.G. Ryan, The composition and origin of subcontinental lithospheric mantle, in: Y. Fei, C.M. Bertka, B.O. Mysen (Eds.), *Mantle Petrology: Field Observations and High-Pressure Experimentation: A Tribute to Francis R. (Joe) Boyd*, Geochemical Society Special Publication, vol. 6, The Geochemical Society, Houston, 1999, pp. 13–45.
- [42] D.G. Pearson, G.M. Nowell, The continental lithospheric mantle reservoir: characteristics and significance as a mantle reservoir, *Proc. R. Soc., A* 360 (2002) 1–28.
- [43] M. Nironen, R. Lahtinen, A. Korja, Paleoproterozoic tectonic evolution of the Fennoscandian shield—comparison to modern analogues, in: R. Lahtinen, A. Korja, K. Arhe, O. Eklund, S.-E. Hjelt, L.J. Pesonen (Eds.), *Lithosphere 2002—Second Symposium on the Structure, Composition and Evolution of the Lithosphere in Finland*. Programme and extended abstracts, Espoo, Finland, Institute of Seismology, University of Helsinki, report S-42, 2002, pp. 95–97.
- [44] C.T. Herzberg, W.S. Fyfe, M.J. Carr, Density constraints on the formation of the continental Moho and crust, *Contrib. Mineral. Petrol.* 84 (1983) 1–5.
- [45] S. MahlburgKay, R.W. Kay, Role of crystal cumulates and the oceanic crust in the formation of the lower crust of the Aleutian arc, *Geology* 13 (1985) 461–464.